J. Fluid Mech. (1996), vol. 325, pp. 357–376

Approximations to wave trapping by topography

By P. G. CHAMBERLAIN AND D. PORTER

Department of Mathematics, The University of Reading, PO Box 220, Whiteknights, Reading RG6 6AX, UK

(Received 22 January 1996)

The trapping of linear water waves over two-dimensional topography is investigated by using the mild-slope approximation. Two types of bed profile are considered: a local irregularity in a horizontal bed and a shelf joining two horizontal bed sections at different depths. A number of results are derived concerning the existence of trapped modes and their multiplicity. It is found, for example, that the maximum number of modes which can exist depends only on the gross properties of the topography and not on its precise shape. A range of problems is solved numerically, to inform and illustrate the analysis, using both the mild-slope equation and the recently derived modified mild-slope equation.

1. Introduction

The existence of trapped modes in linearized water wave theory has been known since the work of Stokes (1846). However, it is only recently that the wide variety of circumstances in which wave trapping can occur has become apparent. Evans & Kuznetsov (1996) give a comprehensive review of recent developments in the general area of water wave trapping.

This paper is concerned with one particular wave trapping mechanism: irregularities in the bed level. To describe the situation we envisage explicitly, we refer to Cartesian coordinates with z directed vertically upwards and the x- and y-axes lying in the undisturbed free surface. We suppose that the bed profile has a constant cross-section in the y-direction, given by $z = -h(x)$. Further, we assume that $h(x)$ takes constant values outside a finite interval, so that either there is a local perturbation on an otherwise horizontal bed or there is a shelf of finite extent joining two horizontal bed sections at different depths. We seek waves of length $2\pi/m$ which propagate in the y-direction with angular frequency σ. Such a wave is said to be trapped if its energy per unit length of the y-axis is finite. In other words, the wave is trapped over the bed undulations and its elevation decays as $|x| \to \infty$. The problem thus posed is an eigenvalue problem, in which either σ or m can be regarded as the eigenvalue parameter, the other being assigned.

Previous work in this area has been principally concerned with the existence of trapped modes and the implied non-uniqueness of solutions of the corresponding forced wave problems, and operator theory provides a natural tool for this purpose. Thus, Jones (1953) established the existence of trapped modes in the presence of a symmetric ridge protruding from a horizontal bed, whilst Garipov (see Lavrentiev & Chabat 1973) considered ridges of arbitrary cross-section.

More explicit information can be obtained if the shallow-water approximation is invoked and this is the basis of an examination of trapped waves given by Mei (1983).

LeBlond & Mysak (1978) consider a number of wave trapping mechanisms for both rotating and non-rotating shallow flows.

In the case of symmetric bedforms, contact may be made with so-called edge waves. Thus, for trapped modes which are also symmetric, a rigid vertical barrier (a 'cliff') may be inserted along the axis of symmetry of the topography, from the bed to the free surface. The waves trapped above the topography then fall into the category described as edge waves. In a recent important paper Bonnet-Ben Dhia & Joly (1993) have considered a range of edge waves, including those in the class just described, and have used operator theory to derive a number of conditions under which such waves can exist.

Here we consider the trapping of waves over topography by invoking the mild-slope approximation. This has the effect of reducing the underlying problem to one of Sturm–Liouville type, allowing numerical computations to be carried out which illustrate the associated analysis. The approximation also permits us to consider the topography, mentioned earlier, which consists of an arbitrary shelf between two different horizontal bed levels and which has evidently not been examined previously in the context of wave trapping.

In a recent re-appraisal of the mild-slope approximation, Chamberlain & Porter (1995*a*) have derived the modified mild-slope equation by using a particular trial function in a variational principle equivalent to the full linear problem. This new equation (which is given explicitly later) reduces to the familiar mild-slope equation if terms which are considered to be small on the basis of the mild-slope approximation ($h' \ll kh$ in the notation given later) are deleted. However, these terms can be significant, as shown by Porter & Staziker (1995) who have also demonstrated that the original mild-slope equation may be used for slopes up to one in one, extending the estimate of one in three given by Booij (1983). Porter & Chamberlain (1996) have recently compared the mild-slope approximation with other approximation methods for wave motion over topography.

We consider a generic approximating equation in §2, which includes the mild-slope and modified mild-slope equations, and use it to establish some general properties of trapped modes. In §3, we examine the special case of periodic topography which is significant in forced wave problems (see, for example, Chamberlain & Porter 1995*b*). The general results of §2 are applied to the mild-slope equation in §4 and lead, for instance, to a bound on the maximum number of trapped modes which can exist for a given frequency, expressed only in terms of the gross properties of the topography. Numerical results are presented in §5 for the mild-slope and modified mild-slope equations and for a number of bed profiles. These results are used to illustrate various aspects of the theory and to give graphical representations of some of the analytic properties.

2. The basic problem

We consider the class of approximations to wave motion over an uneven bed in which the free-surface elevation is given by $\mathrm{Re}\{\eta(x,y)\mathrm{e}^{-\mathrm{i}\sigma t}\}$, where the angular frequency σ is assigned and η satisfies the equation

$$\nabla \cdot u\nabla\eta + v\eta = 0, \tag{2.1}$$

where $\nabla = (\partial/\partial x, \partial/\partial y)$. The functions $u > 0$ and v are given and depend on the undisturbed depth $H(x,y)$ of the fluid. In particular, in regions where the bed is horizontal, u and v are constant with $v = k^2 u$, where k, the wavenumber, is a constant

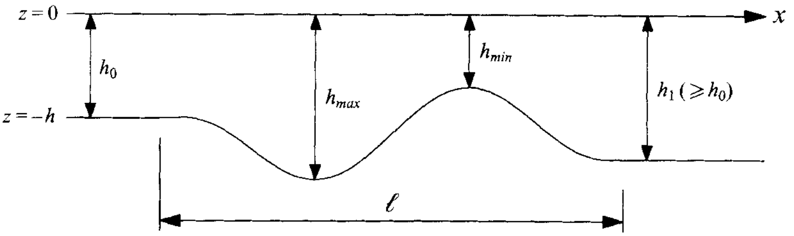

FIGURE 1. Definition sketch.

depending on the depth of the bed. Anticipating the dispersive properties associated with the particular examples of (2.1) we shall refer to later, we assume that $k(H)$ is a decreasing function.

The structure we have described includes the mild-slope equation and the modified mild-slope equation, which we shall refer to explicitly in due course.

We are concerned here with two-dimensional topography in the sense that

$$H(x, y) = h(x) \qquad (-\infty < x < \infty, -\infty < y < \infty).$$

We further assume that $h(x)$ and $h'(x)$ are continuous and that

$$h(x) = \begin{cases} h_0 & (-\infty < x < 0), \\ h_1 & (\ell < x < \infty), \end{cases} \tag{2.2}$$

h_0 and h_1 being constants. Ultimately, we shall consider two basic types of topography: a localized irregularity in an otherwise horizontal bed (so that $h_0 = h_1$), and a shelf of arbitrary profile joining two semi-infinite horizontal bed sections at different depths (taking $h_1 > h_0$ for definiteness in this case).

Figure 1 illustrates the general situation; h_{min} and h_{max} have the obvious definitions (given explicitly in §4) and are referred to repeatedly later. In specific examples considered later h_{max} may be equal to h_1 which, in turn, may be equal to h_0. However, as we shall see, it will be necessary that $h_{min} < h_0$.

The trapped modes we seek are those for which

$$\eta(x, y) = X(x)\mathrm{e}^{\mathrm{i}my}, \tag{2.3}$$

where m is a real number which we can take to be non-negative, and

$$X(x) \to 0, \quad |x| \to \infty. \tag{2.4}$$

We thus have to solve the eigenvalue problem consisting of (2.4) together with (2.1) reduced to the form

$$(uX')' + (v - m^2u)X = 0 \quad (-\infty < x < \infty). \tag{2.5}$$

On each interval where h is constant (2.1) simplifies to

$$X'' + (k^2 - m^2)X = 0,$$

where $k = k(h)$, and (2.2) therefore implies that

$$X(x) = \begin{cases} a_0\mathrm{e}^{\alpha_0 x} & (x < 0), \\ a_1\mathrm{e}^{-\alpha_1 x} & (x > \ell), \end{cases} \tag{2.6}$$

where $\alpha_j = (m^2 - k_j^2)^{1/2}$, $k_j = k(h_j)$ for $j = 0, 1$ and a_0, a_1 are constants. In view of

(2.4) we require

$$m > k_0, \tag{2.7}$$

since $k_0 \geqslant k_1$ by hypothesis.

The core of the problem is thus to find non-trivial solutions of

$$(uX')' + (v - m^2u)X = 0 \quad (0 < x < \ell) \tag{2.8}$$

which match appropriately with (2.6). Clearly, $X(x)$ and $X'(x)$ must be continuous everywhere to ensure continuity of the free surface and its slope. It should be remarked here that a consistent application of the mild-slope approximation requires that the free surface slope be discontinuous at locations where the bed slope is discontinuous (see Porter & Staziker 1995). We have imposed the continuity of $h'(x)$ to eliminate unrealistic free-surface profiles. (In the corresponding scattering problem, with a wave train incident from $x = -\infty$, say, local inaccuracies in the surface profile can be tolerated, as the principal interest is in the far wave field.) The continuity of X and X' used in conjunction with (2.6) gives boundary conditions for (2.8) in the form

$$X'(0) - \alpha_0 X(0) = 0, \quad X'(\ell) + \alpha_1 X(\ell) = 0. \tag{2.9}$$

Some information about the existence of non-trivial solutions of the boundary value problem consisting of (2.8) and (2.9) follows from standard differential equation theory. To exploit this fact, we suppose that $v(x) > 0$ in some subinterval of $[0,\ell]$, at least, and define the positive number M by

$$M^2 = \max\left(\frac{v(x)}{u(x)}\right) \quad (0 \leqslant x \leqslant \ell). \tag{2.10}$$

If we now define λ by

$$m^2 = M^2 - \lambda$$

then (2.8) takes the form

$$(uX')' + (\lambda u - (M^2u - v))X = 0, \tag{2.11}$$

which, with (2.9) also expressed in terms of λ, constitutes a standard Sturm–Liouville problem. We infer (from the treatment given by Ince 1944, for example, who allows for the presence of λ in the boundary conditions) that there are infinitely many positive eigenvalues λ_j which can be arranged in increasing order of magnitude so that

$$0 < \lambda_0 < \lambda_1 < \lambda_2 \cdots.$$

Further, if the corresponding eigenfunctions are denoted by $X_0, X_1, X_2, \ldots$ then $X_j(x)$ has exactly j zeros for $0 < x < \ell$.

The problem in its original form therefore has prospective eigenvalues given by $m_j^2 = M^2 - \lambda_j$ satisfying $M > m_0 > m_1 > m_2 \ldots,$ of which only those which also satisfy (2.7) are admissible. We now see the significance of the assumption $M^2 > 0$ and that the stronger condition $M > k_0$ is actually necessary for the existence of a trapped mode. If this condition is satisfied, appropriate solutions of (2.8) and (2.9) consist of at most the n eigenvalues m_j $(j = 0, 1, 2, \ldots, n-1)$ for some $n \geqslant 1$, where

$$M > m_0 > m_1 > \ldots > m_{n-1} > k_0 \geqslant m_n, \tag{2.12}$$

together with the corresponding eigenfunctions $X_0, X_1, \ldots, X_{n-1}$, where X_j has exactly j zeros.

Of course, we have yet to establish a condition which ensures that $m_0 > k_0$, so that at least one trapped mode can exist. This aspect is most easily dealt with by considering the problem consisting of (2.4) and (2.5). It can readily be shown that the functional

$$J(\xi) = \left(\int_{-\infty}^{\infty} v\xi^2 \mathrm{d}x - \int_{-\infty}^{\infty} u\xi'^2 \mathrm{d}x\right) \Big/ \int_{-\infty}^{\infty} u\xi^2 \mathrm{d}x, \tag{2.13}$$

taken over all 'suitable' real-valued functions $\xi(x)$, is stationary at $\xi = X$ if and only if X satisfies (2.4) and (2.5). The stationary values of $J(\xi)$ are the squares m_j^2 of the eigenvalues, establishing the maximum principle $J(\xi) \leqslant m_0^2$, equality being attained at, and only at, $\xi = X_0$.

We therefore have

$$m_0^2 - k_0^2 \geqslant L(\xi) \equiv \left(\int_{-\infty}^{\infty} (v - k_0^2 u)\xi^2 \mathrm{d}x - \int_{-\infty}^{\infty} u\xi'^2 \mathrm{d}x\right) \Big/ \int_{-\infty}^{\infty} u\xi^2 \mathrm{d}x. \tag{2.14}$$

This characterisation of the problem allows 'weak' solutions of (2.4) and (2.5) to be considered in which $\xi(x)$ is required to be continuous and have a continuous derivative, and such that the integrals in (2.14) converge. At least one trapped mode exists if we can find such a ξ for which $L(\xi) > 0$. Motivated by the need for simplicity and by the fact that the maximizer X_0 of $L(\xi)$ is known to be one-signed, we choose the test function

$$\xi(x) = \begin{cases} \operatorname{sech}(\alpha x) & (x < 0), \\ 1 & (0 \leqslant x \leqslant \ell), \\ \operatorname{sech}\beta(\ell - x) & (x > \ell), \end{cases}$$

where α and β are positive, real parameters. For this ξ, the functional $L(\xi)$ takes the values of

$$L(\alpha, \beta) = \frac{-\frac{1}{3}(u_0\alpha + u_1\beta) + (k_1^2 - k_0^2)u_1\beta^{-1} + \int_0^{\ell} (v - k_0^2 u)\mathrm{d}x}{u_0\alpha^{-1} + u_1\beta^{-1} + \int_0^{\ell} u\mathrm{d}x}$$

for $\alpha > 0$ and $\beta > 0$, where u_0 and u_1 denote the constant values of u for $x < 0$ and $x > \ell$ respectively.

The maximum value of $L(\alpha, \beta)$ can be determined by elementary calculus. The case in which $k_0 = k_1$ is straightforward and it is found that this maximum is positive provided that

$$\int_0^{\ell} (v - k_0^2 u)\mathrm{d}x > 0. \tag{2.15}$$

Indeed, this condition follows directly from $L(\alpha, \beta)$ by inspection. The corresponding calculation is a little more involved for $k_0 > k_1$, leading to the condition

$$\int_0^{\ell} (v - k_0^2 u)\mathrm{d}x > 2u_1[(k_0^2 - k_1^2)/3]^{1/2} \tag{2.16}$$

for the maximum value of $L(\xi)$ to be positive, for the chosen test function.

The inequality (2.16) is therefore a sufficient condition for the existence of at least one trapped mode in the case $h_1 \geqslant h_0$; it reduces to (2.15) if $h_0 = h_1$. We comment on (2.16) later in relation to a specific application of the theory.

Assuming that (2.16) is satisfied, we can obtain an estimate of the maximum number of modes which can exist, by using a comparison theorem in conjunction with (2.8). Let p and q be constants satisfying

$$u \geqslant p > 0, \quad m^2u - v \geqslant q \tag{2.17}$$

in $(0,\ell)$ and let the function $Z(x)$ satisfy

$$pZ'' - qZ = 0 \quad (0 < x < \ell).$$

Then, by Picone's theorem (see, for example, Ince 1944), Z has at least one zero between two consecutive zeros of X. This property follows from the inequality

$$[XZ^{-1}(uZX' - pXZ')]_{x_1}^{x_2} > 0 \tag{2.18}$$

which holds for $0 \leqslant x_1 < x_2 \leqslant \ell$, with $Z(x)$ non-vanishing for $x_1 \leqslant x \leqslant x_2$.

Noting that the inequality $M > m_0$ implies that $q < 0$, we first take the comparison function

$$Z(x) = \sin(\omega x),$$

where $\omega = (-q/p)^{1/2}$ and suppose that

$$N\pi/\omega < \ell \leqslant (N + \tfrac{1}{2})\pi/\omega$$

for some positive integer N. Then Z has exactly N zeros in $(0,\ell)$, located at $x = n\pi/\omega$ $(n = 1, 2 \ldots N)$. Therefore X has at most $N + 1$ zeros in $(0,\ell)$. Suppose, however, that x_1 is a zero of X such that $N\pi/\omega < x_1 < \ell$ and take $x_2 = \ell$. Then, using $X'(\ell) + \alpha_1 X(\ell) = 0$, $Z(\ell) > 0$ and $Z'(\ell) > 0$, we contradict (2.18), concluding that X has no such zero. Therefore X actually has at most N zeros in $(0,\ell)$. In the case

$$(N + \tfrac{1}{2})\pi/\omega < \ell \leqslant (N + 1)\pi/\omega$$

we take the comparison function $Z(x) = \cos(\omega x)$. Using (2.18) it follows that X has no zero in $(0, \pi/2\omega)$ or in $((N + \frac{1}{2})\pi/\omega, \ell)$ and therefore it has at most N zeros in $(0,\ell)$. A similar approach shows that X has no zeros in $(0,\ell)$ if $\ell \leqslant \pi/\omega$. (The single comparison function $\sin(\omega x + \theta)$ with $\pi/2 < \theta < \pi$ encompasses all cases but is a little more intricate to use.)

Recalling that the eigenfunction X_j has j zeros we conclude that if

$$N\pi < \ell(-q/p)^{1/2} \leqslant (N + 1)\pi \quad (N = 0, 1, 2 \ldots) \tag{2.19}$$

then at most $N + 1$ trapped modes can exist. To convert this result into a practical form requires the determination of constants p and q satisfying (2.17); in particular, the inequality $m > k_0$ must be used to deduce q. We remark here that an oscillatory comparison function is not available to obtain an estimate of the minimum number of trapped modes in a similar way, because the maximum value of $m^2u - v$ in $(0,\ell)$ is positive.

An alternative way of obtaining qualitative information about admissible solutions of (2.5) follows from a phase-plane analysis. This approach was used by Mei (1983) in the case of shallow-water theory.

We replace (2.5) by the coupled equations

$$uX' = Y, \quad Y' = (m^2u - v)X \quad (-\infty < x < \infty) \tag{2.20}$$

and note from (2.6) that

$$Y = u_0\alpha_0 X \quad (-\infty < x < 0), \quad Y = -u_1\alpha_1 X \quad (\ell < x < \infty)$$

and that every trajectory in the (X, Y)-plane representing a trapped mode must cut the coordinate axes orthogonally. We choose that part of the trajectory corresponding

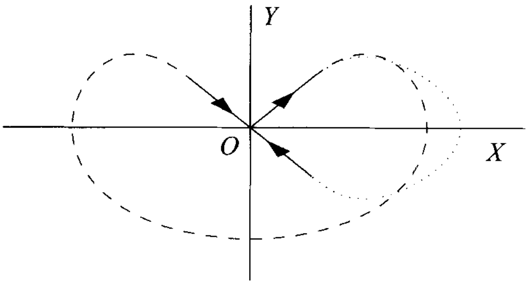

FIGURE 2. Idealized phase portraits of X against $Y = uX'$. Sketch gives examples of how the trajectory departs from the origin in the first quadrant and returns to the origin in the second or fourth quadrants.

to $-\infty < x < 0$ to be in $X > 0$, $Y > 0$; the part corresponding to $\ell < x < \infty$ is then either in $X > 0$, $Y > 0$ or in $X < 0$, $Y > 0$.

For a continuous solution to be possible therefore, Y' must change sign at least twice where $X \neq 0$, implying that $m^2u - v$ must change sign at least twice in the interval $(0, \ell)$. Therefore we must have $\min(m^2u - v) < 0$ in $(0, \ell)$ or $m < M$, using (2.10). We again conclude that $\max(v/u) > 0$ is necessary for a trapped mode to exist and that (if this condition is satisfied) every eigenvalue is such that $k_0 < m_j < M$.

Figure 2 shows typical trajectories for X_0 and X_1 for a simple topography, with, in this case, $m^2u - v$ changing sign exactly twice in $(0, \ell)$. The trajectory representing X_j cuts the Y-axis j times before returning to the origin on one of the two available paths. In other words, the trajectory corresponding to X_{2j} (X_{2j+1}) returns to the origin in the second (fourth) quadrant. These remarks accord with the prediction of Sturm–Liouville theory concerning the number of zeros of X_j. More complicated topography will naturally result in more intricate trajectories, by increasing the number of zeros of $m^2u - v$ in $(0, \ell)$ – see, for example, the problem considered in §5.3.

We conclude this section by giving an alternative version of the problem, in which we normalize the solution of (2.8) and (2.9) by choosing $X(0) = 1$ (noting that there is clearly no non-trivial solution satisfying $X(0) = 0$ and hence $X'(0) = 0$). We then have to solve the initial value problem

$$(uX')' + (v - m^2u)X = 0 \quad (x > 0), \quad X(0) = 1, \quad X'(0) = \alpha_0 \tag{2.21}$$

and ensure that the solution satisfies the the equation

$$\mathscr{F}(m) \equiv X'(\ell) + \alpha_1 X(\ell) = 0. \tag{2.22}$$

This formulation provides the basis for the computations we describe later and allows us to analyse the trapping properties of a certain class of topography, as we show next.

3. Periodic topography

In this section we consider the case in which the depth function h is periodic in the interval $(0, \ell)$. We suppose that $\ell = N_p\mu$ for some $N_p \in \mathbb{N}$ and that $h(x) = h(x + n\mu)$ for $0 \leqslant x \leqslant \mu$ and $n = 1, 2, \ldots, N_p - 1$. This depth profile represents N_p periods of a particular bed shape. Continuity of h and h', taken with (2.2), shows that $h_0 = h(n\mu) = h_1$ for $n = 1, 2, \ldots, N_p - 1$; it follows that $\alpha_0 = \alpha_1$.

We recall that our objective is to find eigenvalues m_j such that there exist non-trivial solutions of the initial value problem (2.21) subject to the eigenvalue constraint (2.22).

Our aim is to avoid the computationally expensive task of solving (2.21) in the whole interval $0 \leqslant x \leqslant N_p\mu$. Chamberlain & Porter (1995*b*) have shown how this objective can be achieved for wave scattering problems and here their approach is adapted to the eigenvalue problem in hand. We show that only the solutions of a simple pair of initial value problems, in the smaller interval $0 \leqslant x \leqslant \mu$, are required. Suppose that

$$\begin{aligned}(u\chi_j')' + v\chi_j &= m^2 u\chi_j \quad (x > 0, \quad j = 0, 1),\\ \chi_0(0) &= \chi_1'(0) = 1,\\ \chi_0'(0) &= \chi_1(0) = 0,\end{aligned}$$

from which we easily see that $X = \chi_0 + \alpha_0\chi_1$, provided that the eigenvalue constraint

$$\mathscr{F}^{(N_p)}(m) = \chi_0'(N_p\mu) + \alpha_0\chi_1'(N_p\mu) + \alpha_0\left(\chi_0(N_p\mu) + \alpha_0\chi_1(N_p\mu)\right) = 0 \tag{3.1}$$

is satisfied. The superscript notation adopted in (3.1) indicates how many periods are under consideration.

Periodicity of h implies that u and v are also periodic. It follows that $\chi_j(x + n\mu)$ $(j = 1, 2)$ is a linear combination of $\chi_0(x)$ and $\chi_1(x)$ for $x \in [0, \mu]$ since they are solutions of the same differential equation. Indeed, it follows that

$$\left.\begin{aligned}\chi_0(x + n\mu) &= \chi_0(n\mu)\chi_0(x) + \chi_0'(n\mu)\chi_1(x)\\ \chi_1(x + n\mu) &= \chi_1(n\mu)\chi_0(x) + \chi_1'(n\mu)\chi_1(x)\end{aligned}\right\} \quad (0 \leqslant x \leqslant \mu), \tag{3.2}$$

for $n = 1, 2, \ldots, N_p - 1$.

Let $a_n = \chi_0(n\mu)$, $b_n = \chi_0'(n\mu)$, $c_n = \chi_1(n\mu)$ and $d_n = \chi_1'(n\mu)$ for brevity. Substituting $x = \mu$ into equations (3.2), and their derivatives, yields

$$\left.\begin{aligned}a_{n+1} &= a_1 a_n + c_1 b_n, \qquad & b_{n+1} &= b_1 a_n + d_1 b_n,\\ c_{n+1} &= a_1 c_n + c_1 d_n, & d_{n+1} &= b_1 c_n + d_1 d_n,\end{aligned}\right\} \quad (n \geqslant 1), \tag{3.3}$$

where, as a consequence of our assumed initial conditions, we have $a_0 = d_0 = 1$ and $b_0 = c_0 = 0$.

Rearranging (3.3) gives

$$a_{n+2} - 2\gamma a_{n+1} + a_n = 0$$

where $\gamma = \frac{1}{2}(a_1 + d_1)$. The quantities b_n, c_n and d_n satisfy the same difference equation which is readily solved to show that

$$\left.\begin{aligned}a_n &= a_1\sigma_n - \sigma_{n-1}, \qquad & b_n &= b_1\sigma_n,\\ c_n &= c_1\sigma_n & d_n &= d_1\sigma_n - \sigma_{n-1},\end{aligned}\right\} \quad (n \geqslant 1), \tag{3.4}$$

where $\sigma_n = \sin n\theta / \sin\theta$ in which $\theta = \cos^{-1}\gamma \in \mathbb{C}$ is defined such that $0 \leqslant \mathrm{Re}(\theta) \leqslant \pi$ and $\mathrm{Im}(\theta) \geqslant 0$. (The case in which $\theta = 0$ can be dealt with separately and it is easy to show that $\sigma_n = n$.)

Use of (3.4) allows us to write the eigenvalue equation (3.1) as

$$\mathscr{F}^{(N_p)}(m) = \mathscr{F}^{(1)}(m)\sigma_{N_p} - 2\alpha_0\sigma_{N_p - 1}, \tag{3.5}$$

from which it is clear that solutions of the differential equation are only required for $0 < x \leqslant \mu$. The eigenfunction $X = \chi_0 + \alpha_0\chi_1$ can also be found from solutions on the smaller interval, for (3.4) used in conjunction with (3.2) implies that

$$X(x + n\mu) = \{X(\mu)\chi_0(x) + X'(\mu)\chi_1(x)\}\,\sigma_n - X(x)\sigma_{n-1}$$

in which $n = 1, 2, \ldots, N_p - 1$ and $0 \leqslant x \leqslant \mu$.

There is a special case which is of interest here. If $a_1 = d_1 = 1$ and $b_1 = c_1 = 0$ it follows immediately that $\theta = 0$ and also that $a_n = d_n = 1$, $b_n = c_n = 0$ for all $n = 0, 1, 2, \ldots, N_p$. In this case $\chi_0(x)$, $\chi_1(x)$ and consequently $X(x)$ are periodic (with period μ) for $x \in [0, \ell]$, i.e. each period of the bedform has an identical free-surface profile above it.

Finally in this section we note that the result concerning an upper bound on the number of trapped modes given by equation (2.19) carries over to periodic beds in a trivial way. The quantities p and q in equation (2.19) are independent of N_p; indeed only $\ell = N_p\mu$ depends on the number of periods and it does so in an explicit way.

4. Application to the mild-slope approximation

The mild-slope equation, originally derived by Berkoff (1973) and independently by Smith & Sprinks (1973), is an example of (2.1). It arises by approximating the vertical structure of the fluid motion and averaging over the fluid depth in a process which can be formalized by using Galerkin's method (see Chamberlain & Porter 1995*a*). For the two-dimensional topography under consideration here, with $h(x)$ denoting the local undisturbed depth, the coefficients u and v can conveniently be expressed in the forms

$$u(h) = \tanh(kh)\{1 + 2kh\operatorname{cosech}(2kh)\}/2k, \quad v(h) = k^2 u(h), \tag{4.1}$$

where the local wavenumber $k(h)$ is defined implicitly by the dispersion relation

$$\nu = k\tanh(kh). \tag{4.2}$$

We regard $\nu = \sigma^2/g$ as an assigned parameter and it is easily checked that $k(h)$ is a decreasing function at each value of ν, as assumed in §2. The derivation of the mild-slope equation assumes that $h' \ll kh$ for all x.

Referring to (2.10) we see that, in this application, $M = \max\{k(h(x)) : 0 \leqslant x \leqslant \ell\}$ and therefore the necessary condition $M > k_0$ for a trapped mode to exist can be expressed as

$$h_{min} < h_0, \quad h_{min} = \min\{h(x) : 0 \leqslant x \leqslant \ell\}. \tag{4.3}$$

Thus, a trapped wave is possible only if part of the bed projects above the (higher of the two) bed levels at infinity.

The sufficient condition (2.16) for the existence of at least one trapped mode takes the slightly modified form

$$\int_0^\ell u(k^2 - k_0^2)\mathrm{d}x > 2u_1\left[(k_0^2 - k_1^2)/3\right]^{1/2}. \tag{4.4}$$

This shows that a trapped wave exists above any elevation on an otherwise flat bed since $h(x) < h_0$ implies that $k > k_0$ and the right-hand side of (4.4) reduces to zero in this case. A trapped wave will also exist if there is a depression in a horizontal bed, provided that there is also a compensating elevation which makes the integral on the left of (4.4) positive. In this case, and for $h_0 \neq h_1$, the condition (4.4) can be checked numerically for a given bedform and a given value of ν. However, it is more directly revealing in certain limits. Thus, for large νh, we find from (4.1) and (4.2) that

$$k = \nu\{1 + \mathrm{e}^{-2\nu h} + O(\mathrm{e}^{-4\nu h})\}, \quad u = \{1 + O(\nu h\mathrm{e}^{-2\nu h})\}/2\nu.$$

To leading order for large νh_0, therefore, (4.4) takes the form

$$\frac{1}{h_0}\int_0^{\ell}\{e^{2\nu(h_0-h)}-1\}dx > \frac{2e^{\nu h_0}}{\nu h_0}\left[\tfrac{2}{3}(1-e^{-2\nu(h_1-h_0)})\right]^{1/2}. \tag{4.5}$$

In the case $h_0 = h_1$ this inequality reduces to

$$\frac{1}{\ell}\int_0^{\ell} e^{2\nu(h_0-h)}dx > 1,$$

which is automatically satisfied for sufficiently large νh_0 by virtue of (4.3). Thus $h_{min} < h_0$ is both necessary and sufficient for the existence of at least one trapped mode, if νh_0 is large enough. This result is given, for edge waves and using full linear theory, by Bonnet-Ben Dhia & Joly (1993). We also note that, since $M - k_0 = k(h_{min}) - k_0 \to 0$ as $\nu h_0 \to \infty$, the trapped modes we are seeking here (having smooth free-surface profiles) are formally excluded in this limit, because of (2.12).

We also find from (4.5) that the condition $h_{min} < \frac{1}{2}h_0$ is sufficient to satisfy (4.4) and ensure that at least one trapped mode exists, for large enough νh_0 and *any* $h_1 > h_0$.

The case in which $\nu h \ll 1$ corresponds to shallow-water theory and (4.1) and (4.2) can be approximated, to leading order, by

$$u = h, \quad v = \nu, \tag{4.6}$$

which reduce (4.4) to the form

$$\int_0^{\ell}(h_0 - h)dx > 2\left[h_0 h_1(h_1 - h_0)/3\nu\right]^{1/2}.$$

For $h_0 = h_1$ and $\nu h_0 \ll 1$, the sufficient condition (4.4) can therefore be expressed as

$$\int_{-\infty}^{\infty}(h_0 - h)dx > 0. \tag{4.7}$$

Bonnet-Ben Dhia & Joly (1993) have proved, again for edge waves and using full linear theory, that (4.7) is necessary and sufficient for a trapped mode to exist at *every* $\nu > 0$.

To apply (2.19) in the present case we note by using (2.7) and (4.1) that

$$m^2 u - v > (k_0^2 - k^2)u.$$

It can be shown that the function $(k_0^2 - k^2)u$ increases with h at each value of ν and, referring to (2.17), we can therefore take

$$q = (k_0^2 - k^2(h_{min}))u(h_{min}).$$

To assign p we observe that $u(h) \to 0$ as $h \to 0$ and $u(h) \to 1/2\nu$ as $h \to \infty$. We can also show that $u(h)$ has a maximum value (where $3\sinh(2kh) = 2kh(\cosh(2kh) - 2)$). Thus the minimum value of $u(h)$ for a given bedform $h(x)$ is

$$p = \min(u(h_{min}), u(h_{max})), \quad h_{max} = \max\{h(x) : 0 \leqslant x \leqslant \ell\}.$$

It now follows from (2.19) that at most $N + 1$ trapped modes can exist if

$$N\pi < \ell\Omega/h_0 \leqslant (N+1)\pi \quad (N = 0, 1, 2, \ldots), \tag{4.8}$$

where Ω is the dimensionless quantity defined by

$$\Omega^2 = h_0^2 u(h_{min})(k^2(h_{min}) - k_0^2)/\min(u(h_{min}), u(h_{max})). \tag{4.9}$$

We note that, as Ω depends only on the gross properties of the topography, the maximum number of modes is the same for every topography having the same values of h_{min}/h_0 and h_{max}/h_0, for fixed ℓ/h_0 and νh_0, and this maximum number increases as ℓ/h_0 increases, with the other parameters held constant. Further, using the stated properties of k, u and $(k_0^2-k^2)u$, it follows from (4.9) that Ω, and therefore the maximum number of modes, remains the same or increases as h_{min}/h_0 decreases and as h_{max}/h_0 increases, in each case with the other parameters remaining constant. We also see from (4.8) that, for every topography, there is at most one mode if ℓ/h_0 is small enough.

To examine the effects of frequency changes on a fixed topography we note that

$$\Omega^2 \simeq 2(\nu h_0)^2(\mathrm{e}^{-2\nu h_{min}} - \mathrm{e}^{-2\nu h_0})$$

for large νh_0. Thus, at most one trapped mode can exist if νh_0 is sufficiently large. Taking this observation with our earlier remarks, we have shown that, if $h_{min} < h_0$, one and only one trapped mode can exist for large νh_0, in the case $h_0 = h_1$.

Using the approximations (4.6) we have

$$\Omega^2 \simeq \nu h_0(h_0 - h_{min})/h_{min}$$

for small νh_0, so that at most one trapped mode can exist, for any topography, if νh_0 is small enough.

Further, since $\Omega > 0$ for $0 < \nu h_0 < \infty$ and $\Omega \to 0$ as $\nu h_0 \to 0$ and as $\nu h_0 \to \infty$, then it has at least one maximum value for fixed h_{min}/h_0, h_{max}/h_0 and ℓ/h_0. It follows that there is at least one frequency band within which a given topography can support the largest number of trapped modes. Numerical evidence indicates that there is only one such band; this can be confirmed analytically from (4.9) in the simpler case for which $u(h_{min}) \leqslant u(h_{max})$.

Chamberlain & Porter (1995*a*) have recently derived the modified mild-slope equation which also has the form of (2.1), with $u(h)$ and $k(h)$ still given by (4.1) and (4.2), respectively, but with v replaced by

$$v = k^2u + u^{(1)}h'' + u^{(2)}h'^2, \tag{4.10}$$

in the one-dimensional context. Here

$$u^{(1)}(h) = \frac{\mathrm{sech}^2(kh)}{4(K+\sinh(K))}\left\{\sinh(K) - K\cosh(K)\right\},$$

$$u^{(2)}(h) = \frac{k\,\mathrm{sech}^2(kh)}{12(K+\sinh(K))^3}\Big\{K^4 + 4K^3\sinh(K) - 9\sinh(K)\sinh(2K) + 3K(K+2\sinh(K))(\cosh^2(K) - 2\cosh(K) + 3)\Big\},$$

in which $K = 2kh$. The additional terms arising in v are small on the basis of the mild-slope approximation $h'/kh = O(\epsilon)$ with $X'/kX = O(1)$, where $\epsilon \ll 1$. Nevertheless, these terms increase the range of slopes over which the mild-slope approximation is applicable (see Porter & Staziker 1995). Because of the additional complication introduced by (4.10), we have confined ourselves to a numerical comparison of the mild-slope and modified mild-slope equations, which is remarked on in the following section.

5. Numerical procedure and results

We briefly describe the computational procedure that has been implemented to produce the results presented in this section. It is convenient for this purpose to use the function $Y = uX'$ so that the initial value problem (2.21) may be written as the first-order system $\boldsymbol{y}'(x) = \boldsymbol{f}(x, \boldsymbol{y})$ where $\boldsymbol{y} = (uX, Y)^T$ and $\boldsymbol{f} = (Y, (m^2u - v)X)^T$ with initial condition $\boldsymbol{y}(0) = (1, \alpha_0 u(0))^T$. Approximation methods for such initial value problems are well documented (see Lambert 1992, for example) and are not discussed here.

The eigenvalue equation to be satisfied is given by (2.22) and may now be written in the form

$$u(\ell)\mathscr{F}(m) = Y(\ell) + \alpha_1 u(\ell) X(\ell) = 0.$$

It is therefore clear that the problem in hand is the familiar one of finding roots m_j of the nonlinear equation $\mathscr{F}(m) = 0$ (recall that $u(\ell) \neq 0$). As noted in §2 we are only interested in zeros of $\mathscr{F}$ which lie in the interval (k_0, M).

The numerical procedure adopted is to scan the interval (k_0, M) for pairs of points between which $\mathscr{F}$ changes sign. (It is a consequence of the differential equation theory referred to in §2 that the zeros of $\mathscr{F}$ are simple.) Each evaluation of $\mathscr{F}$ requires us to approximate the solution of the first-order system described above. Pairs of bracketing points, when found, are used in an application of the well-known *regula falsi* method (see, for example, Phillips & Taylor 1973, p. 157 *et seq*) to converge to each eigenvalue.

The numerical results presented are for a selection of bed topographies, these being localized elevations with the property that $h_0 = h_1$ and one example in which $h_0 < h_1$. The results obtained for these bed shapes are typical of those for a wide range of problems and by concentrating on a small selection we are better able to analyse in detail the problems that are considered.

The first example we consider is that of a symmetric cosine elevation. Values of m_j/v are given for three choices of the (dimensionless) parameters $v\ell$ and vh_0. It is verified that the number of eigenvalues does indeed depend on these parameters.

The second example concerns a topography joining two regions of different depths. For the choice of parameters considered phase portraits of X_j against Y_j are given as well as free-surface plots of the eigenfunctions X_j.

In §5.3 we employ the replication formulae derived in §3 to consider a topography composed of six repetitions of an asymmetric elevation.

In §5.4 and §5.5 we present examples which verify the predictions arising from equation (2.19) concerning an upper bound on the number of trapped modes.

5.1. *A symmetric elevation*

Here we consider the depth profile

$$h(x) = h_0\left(1 - \epsilon + \epsilon\cos(2\pi x/\ell)\right) \quad (0 \leqslant x \leqslant \ell)$$

which represents a symmetric elevation for which $h_{min} = h_0(1 - 2\epsilon)$. For the purposes of results presented in this subsection we consider $\epsilon = \frac{1}{10}$.

Table 1 gives results corresponding to three choices of the dimensionless parameters $v\ell$ and vh_0 using both the mild-slope equation and the modified mild-slope equation. In each case we give all $m_j \in (k_0, M)$ (scaled with respect to v for greater generality) and note that the results obtained are very similar for the modified and unmodified mild-slope equations. This is to be expected, for the quantity h'/kh (supposed to be small in the mild-slope approximation) attains the maximum values 0.03, 0.008 and 0.002 respectively (to 1 significant figure) for the three parameter sets considered. Indeed it is verified in the table that the smaller h'/kh is the smaller the difference

$\nu\ell, \nu h_0 =$	2,0.1		14,0.2		12,0.05	
	MSE	MMSE	MSE	MMSE	MSE	MMSE
m_0/ν	3.31604	3.31557	2.51610	2.51599	4.96966	4.96964
m_1/ν			2.42196	2.42189	4.84908	4.84907
m_2/ν			2.34675	2.34675	4.73876	4.73874
m_3/ν					4.64054	4.64054
m_4/ν					4.55838	4.55838
m_5/ν					4.50975	4.50975

TABLE 1. Scaled eigenvalues m_j/ν for the symmetric elevation and for a selection of parameter values. Results are given for the mild-slope equation (MSE) and the modified mild-slope equation (MMSE).

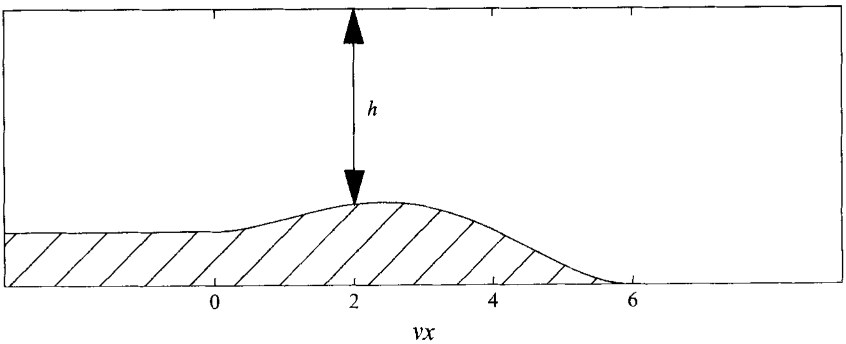

FIGURE 3. Depth profile joining two different depths used in §5.2.

between the two sets of results. Similar evaluations have been carried out for the other examples given below.

5.2. *A shelf joining two different depths*

Consider

$$h(x) = h_0 - \frac{h_0 - h_1}{2\alpha - 1}(x/\ell)^2 \left(3(x/\ell)^2 - 4(1+\alpha)x/\ell + 6\alpha\right) \quad (0 \leqslant x \leqslant \ell)$$

in which $0 < \alpha < \frac{1}{2}$ and $h_1 > h_0$. This profile represents a smooth transition from the depth h_0 to the greater depth h_1 and is such that the minimum depth occurs at $x/\ell = \alpha$. Here we will consider the case in which $h_1/h_0 = 1.25$ and $\alpha = 0.4$. This depth profile is shown in figure 3. The problem is fully prescribed once we choose $\nu h_0 = 0.04$ and $\nu\ell = 6$. In this example we will use the modified mild-slope equation.

With these choices our numerical routine gives us upper and lower bounds on the eigenvalues as $M = 5.38568\nu$ and $k_0 = 5.03357\nu$ respectively. We further find that in this case there are two eigenvalues: $m_0 = 5.27026\nu$ and $m_1 = 5.07246\nu$.

Figure 4 shows the phase portraits of X against $Y = uX'$ for each of the eigenvalues (cf. figure 2). We see that the behaviour predicted in §2 is verified here. Figure 5 shows the corresponding plots of X against the (scaled) independent variable νx. A portion of the exponential solution in $(-\infty, 0] \cup [6, \infty)$ is presented in each case and is shown to join smoothly with the numerically generated solution in $[0, 6]$. We note that the prediction that the function X_j will have exactly j zeros is verified in this example.

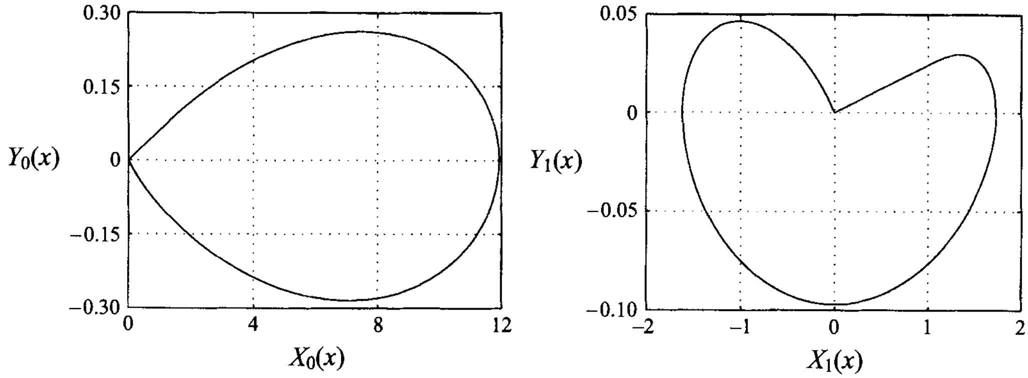

FIGURE 4. Phase portraits corresponding to the two modes for the shelf problem.

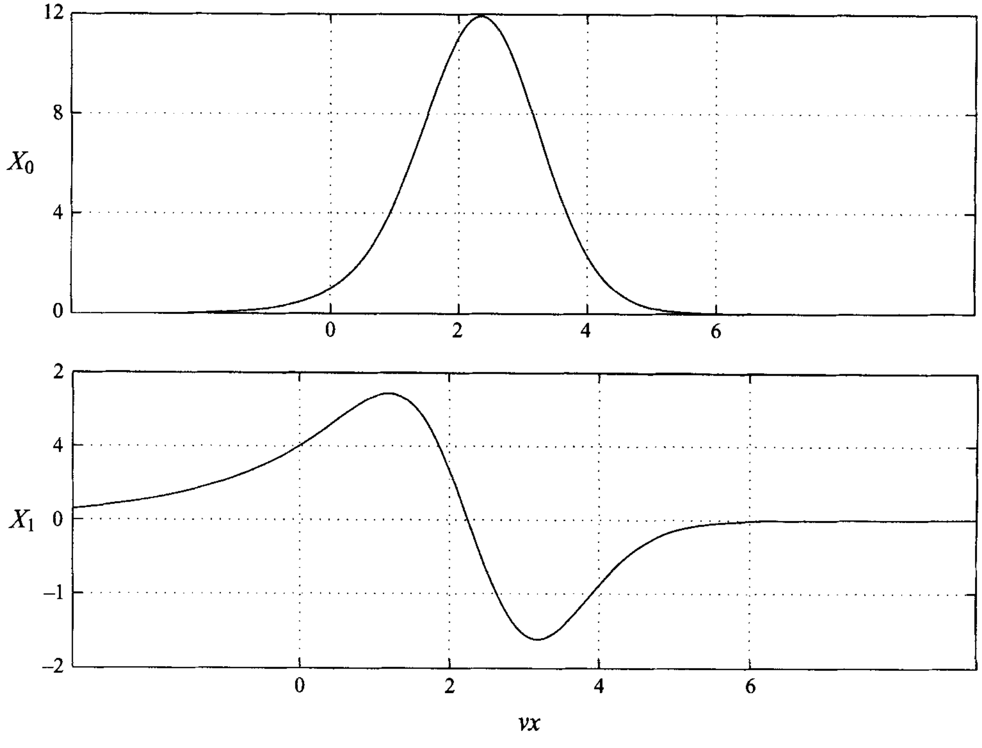

FIGURE 5. Eigenfunction plots $X_j(\nu x)$ corresponding to the two admissible eigenvalues.

5.3. *Repeated asymmetric elevations*

Now we consider a bed that is periodic in the interval $0 \leqslant x \leqslant \ell$. Thus we set $\ell = N_p\mu$ and, for this example, choose a typical period to be given by

$$h(x) = h_0\left(1 - \epsilon + \epsilon\cos(2\pi(x/\mu)^2)\right) \quad (0 \leqslant x \leqslant \mu).$$

We choose $\epsilon = \frac{1}{10}$ so that at its peak the bed shape occupies 20% of the average quiescent depth. Thus, each period is an asymmetric version of the profile considered in §5.1.

In this subsection we will again only consider one set of parameters and examine the

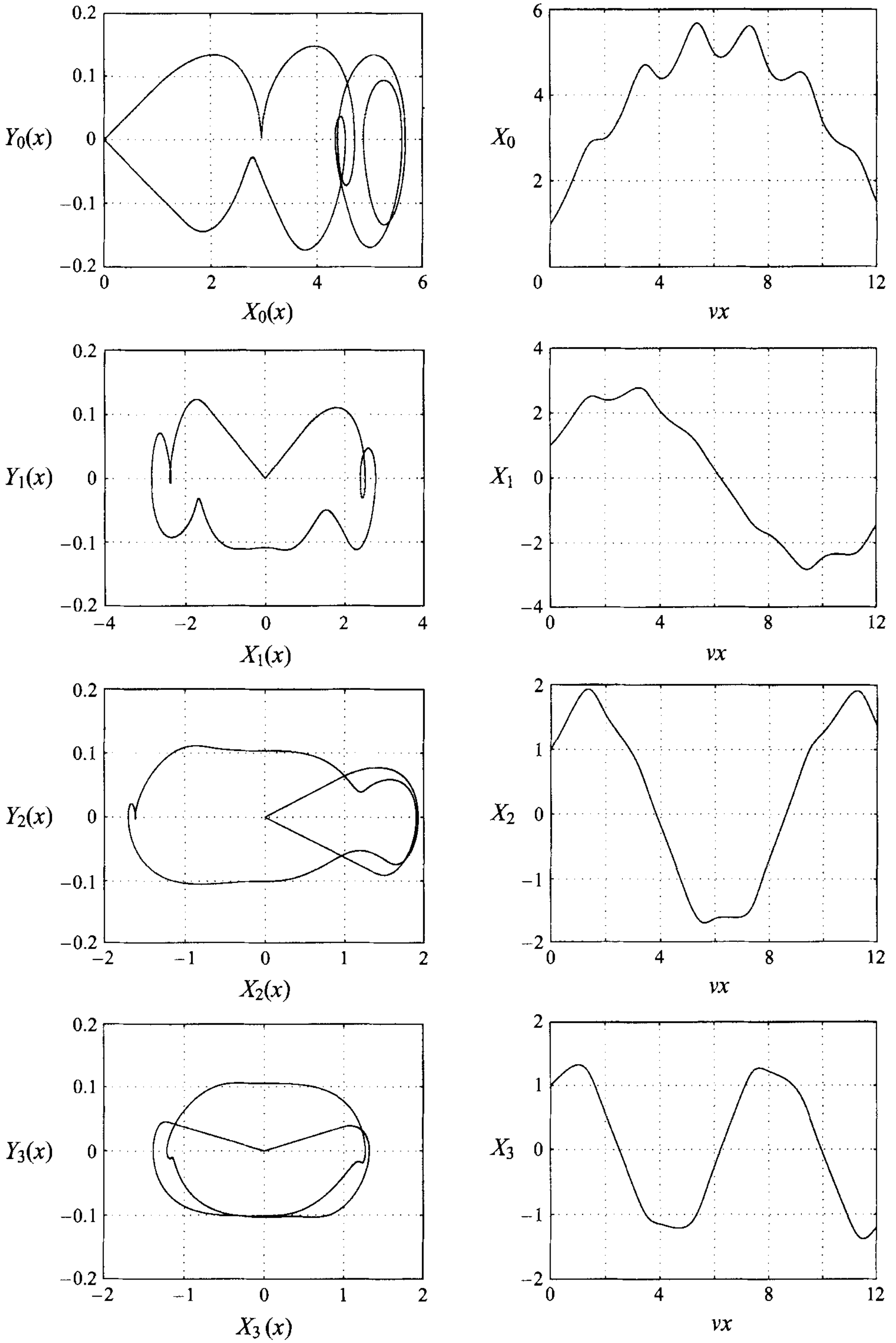

FIGURE 6. Phase portraits and free-surface plots for six periods of the asymmetric profile.

results obtained in detail. Let $\nu h_0 = 0.1$, $\nu\mu = 2$ and $N_p = 6$ (so that $\nu\ell = 12$). We shall carry out our analysis of this problem using the modified mild-slope equation. Using the methods described in §3 we find that there are four eigenvalues: $m_0 = 3.34328\nu$, $m_1 = 3.32188\nu$, $m_2 = 3.28688\nu$ and $m_3 = 3.24069\nu$. Figure 6 shows phase portraits and, alongside, the free-surface plots X_j $(j = 0, 1, 2, 3)$. In this case we have only presented the numerically generated part of X but it has been checked separately that these functions join the exponentially decaying part of the solution smoothly. Indeed, this fact can be seen from the corresponding phase portraits on which the trajectories for $-\infty < x < \infty$ are shown.

5.4. *Three depth profiles*

Consider the three depth profiles

$$\begin{aligned} h^{(1)}(x) &= h_0(1 - \epsilon + \epsilon\cos(2\pi x/\ell)), \\ h^{(2)}(x) &= h_0(1 - \epsilon + \epsilon\cos(4\pi x(\ell - x)/\ell^2)), \\ h^{(3)}(x) &= h_0(1 - \epsilon + \epsilon\cos(\pi\sin(2\pi x(\ell - x)/\ell^2))). \end{aligned}$$

It is readily verified that $\min(h^{(j)}) = h_0(1-2\epsilon)$ $(j = 1, 2, 3)$ and that for each $x \in (0, \ell)$ $h^{(j)}(x) \leqslant h^{(j-1)}(x)$ $(j = 2, 3)$. The hump defined by $h^{(j)}$ is bigger for larger j. These examples are, of course, artificial but they do serve to make an interesting point.

Here we shall put $\epsilon = \frac{1}{10}$ and use the mild-slope equation for which the corresponding theory has been developed explicitly in §4.

We have already observed that equation (2.19), which gives an upper bound on n, the number of trapped modes, takes into account only the gross properties of the underlying depth profile. The functions $h^{(j)}$ above are such that the quantities p and q appearing in (2.19) are independent of j for the mild-slope equation. It is intuitive to expect that the upper bound is tighter the larger j is since in this case approximating u by the constant p and $m^2u - v$ by the negative constant q is 'giving less away'. This subsection serves to confirm that intuition.

Figure 7(a) gives numerically generated data showing values of n for $h^{(1)}$ for a range of values of h_0 and ℓ. The white region corresponds to parameter sets for which only one trapped mode exists. The palest grey region corresponds to $n = 2$, and so on. Figures 7(b) and 7(c) present similar data, but for $h^{(2)}$ and $h^{(3)}$ respectively.

The fourth plot presents those points in the $(\nu\ell, \nu h_0)$-plane at which the upper bound given by equation (2.19) increases by one. For each νh_0 therefore, the position of the curve gives a lower bound on the value of $\nu\ell$ for which this increase occurs. The fact that this *is* a lower bound is verified by comparison with the other three diagrams. It is clear that the estimate given by (2.19) is accurate where n is small. Where n is large it is also rapidly varying and the estimate does predict this rapid variation.

Notice that the predicted curves are better approximations to the edges of the shaded regions for $h^{(j)}$ the larger j is. This fact verifies our earlier prediction.

5.5. *Further examples*

Towards the end of §4 a number of properties were established, based on equation (2.19), concerning cases in which there is at most one trapped mode. (These properties depend on the values of νh_0 and ℓ/h_0 and this influences how numerical data are presented later.) Here we verify those predictions for the depth profile considered in §5.2.

Figure 8 is similar in intent to figure 7(d) in that parameter space is divided into regions according to the upper bound on n, provided by equation (2.19). Guided by

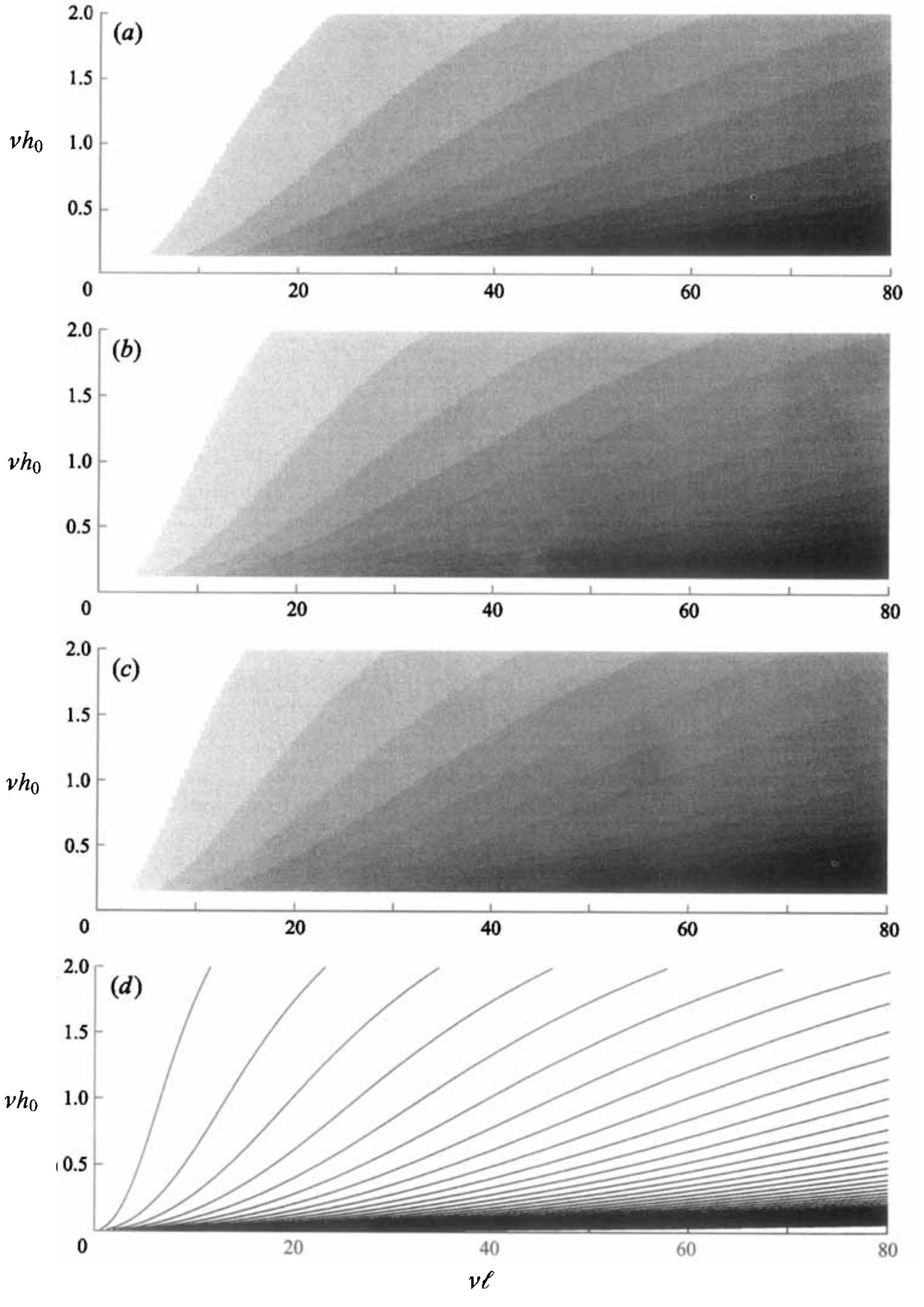

FIGURE 7. Plots (a–c) indicate values of n, the number of admissible eigenvalues, for a range of the dimensionless parameters $\nu\ell$ and νh_0 for the depth profiles described in the text. Plot (d) shows the position of an analytic lower bound on $\nu\ell$ for the positions where n increases.

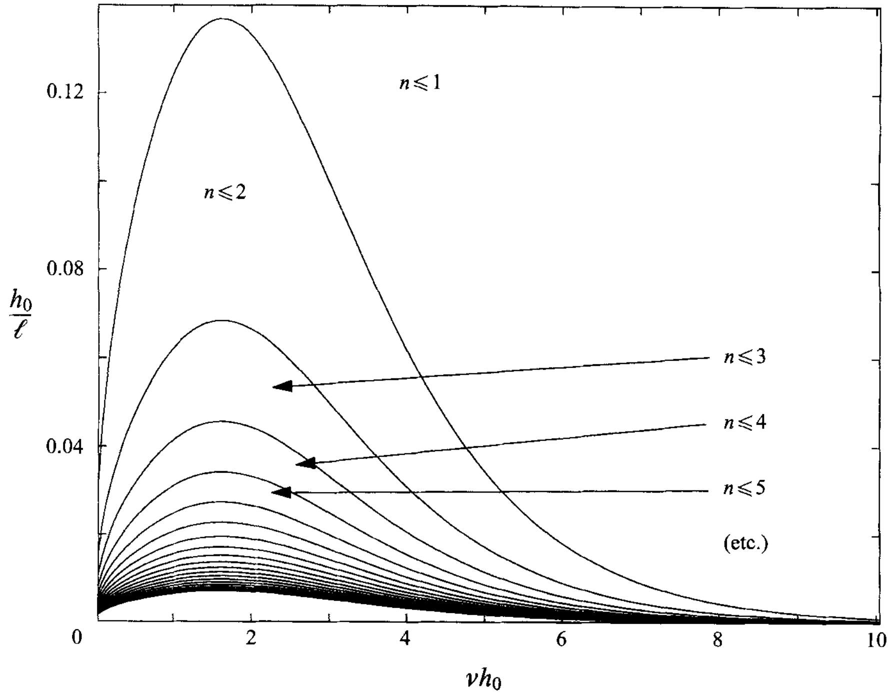

FIGURE 8. Upper bounds on n, the number of trapped modes, for a range of the dimensionless parameters h_0/ℓ and νh_0.

the observation of the preceding paragraph, in this case we consider the dimensionless parameters νh_0 and h_0/ℓ. The contours become closer the smaller h_0/ℓ is and only the first few are presented.

The first thing we note from figure 8 is that there is clearly a value of h_0/ℓ above which there cannot be more than one trapped mode. For example, it is clear from the figure that if $h_0/\ell > 0.14$ then there will be, at most, one trapped mode irrespective of the value taken by the other parameter. This observation agrees with the comment made in §4 that for every topography, there is at most one mode if ℓ/h_0 is small enough.

Furthermore it is evident that, for any h_0/ℓ, there is only one mode for small νh_0 and large νh_0 since the uppermost of the contours in figure 8 approaches zero in both these cases. This is in agreement with earlier results.

6. Conclusions

Wave modes trapped over a class of topography have been investigated by using the mild-slope approximation. In particular, an analysis of the mild-slope equation has led to the following results.

(*a*) For a trapped mode to exist, it is necessary that

$$h_{min} < h_0 \leqslant h_1.$$

This condition is also sufficient for large enough νh_0.

(*b*) For a trapped mode to exist for any ν, it is sufficient that

$$\int_0^{\ell} u(k^2 - k_0^2)\mathrm{d}x > 2u_1 \left[(k_0^2 - k_1^2)/3\right]^{1/2}.$$

This condition is satisfied by every elevation on a horizontal bed. It is also satisfied if there is a depression in the bed (of infinite extent if $h_1 > h_0$) provided that its effect is compensated by a 'large enough' elevation.

(*c*) At most $N + 1$ trapped modes can exist if

$$N\pi < \ell\Omega/h_0 \leqslant (N+1)\pi \quad (N = 0, 1, 2, \ldots), \tag{6.1}$$

where Ω, which depends only on the overall properties h_{min}, h_{max}, h_0 and ℓ of the topography and on the frequency through ν, is given by (4.9). The maximum number of modes remains the same or increases as h_{min} decreases with h_{max} fixed and as h_{max} increases with h_{min} fixed; it increases with ℓ for fixed maximum and minimum depths of the topography. If νh_0 is small, at most one mode can exist. For a fixed topography, there is a finite frequency band which may support a maximum number of trapped waves.

With the exception of (6.1), these results remain valid for edge waves along a cliff. In this case $h_0 = h_1$ and only the symmetric trapped modes transfer to edge modes.

A selection of trapped-mode wavenumbers and the corresponding free-surface profiles has been given for certain bedforms, together with graphical representations of other aspects of the theory. On the basis of the performance of the mild-slope and modified mild-slope equations in wave scattering problems (see, for example, Porter & Staziker 1995), it is anticipated that the present calculations provide a good approximation to the wave modes given by full linear theory.

REFERENCES

BERKHOFF, J. C. W. 1973 Computation of combined refraction–diffraction. *Proc. 13th Intl Conf. on Coastal Engng, July 1972, Vancouver, Canada*, pp. 471–490. ASCE.

BONNET-BEN DHIA, A.-S. & JOLY, P. 1993 Mathematical analysis of guided water waves. *SIAM J. Appl. Maths* **53**, 1507–1550.

BOOIJ, N. 1983 A note on the accuracy of the Mild-Slope equation. *Coastal Engng* **7**, 191–203.

CHAMBERLAIN, P. G. & PORTER, D. 1995*a* The modified mild-slope equation. *J. Fluid Mech.* **291**, 393–407.

CHAMBERLAIN, P. G. & PORTER, D. 1995*b* Decomposition methods for wave scattering by topography with application to ripple beds. *Wave Motion* **22**, 201–214.

EVANS, D. V. & KUZNETSOV, N. 1996 Trapped modes. In *Gravity Waves on Water of Finite Depth* (ed. J. N. Hunt). Computational Mechanics (to appear).

INCE, E. L. 1944 *Ordinary Differential Equations*. Dover.

JONES, D. S. 1953 The eigenvalues of $\nabla^2 u - \lambda u = 0$ when the boundary conditions are given on semi-infinite domains. *Proc. Camb. Phil. Soc.* **49**, 668–684.

LAMBERT, J. D. 1992 *Numerical Methods for Ordinary Differential Systems*. Wiley.

LAVRENTIEV, M. A. & CHABAT, B. V. 1973 *Effets Hydrodynamiques et Modeles Mathematique*. Mir, Moscow.

LEBLOND, P. H. & MYSAK, L. A. 1978 *Waves in the Ocean*. Elsevier.

MEI, C. C. 1983 *The Applied Dynamics of Ocean Surface Waves*. Wiley.

PHILLIPS, G. M. & TAYLOR, P. J. 1973 *Theory and Applications of Numerical Analysis*. Academic Press.

PORTER, D. & CHAMBERLAIN, P. G. 1996 Linear wave scattering by two-dimensional topography. In *Gravity Waves on Water of Finite Depth* (ed. J. N. Hunt). Computational Mechanics (to appear).

Porter, D. & Staziker, D. J. 1995 Extensions of the mild-slope approximation. *J. Fluid Mech.* **300**, 367–382.

Smith, R. & Sprinks T. 1975 Scattering of surface waves by a conical island. *J. Fluid Mech.* **72**, 373–384.

Stokes, G. G. 1846 Report on recent researches in hydrodynamics. *Report on 16th Mtg Brit. Assoc. Adv. Science, Southampton, pp. 1–20.* Murrey, London. Also in *Mathematical and Physical Papers,* vol. I, p. 167, Cambridge University Press, 1880.